JOURNAL OF MATERIALS SCIENCE **35** (2000) 1555–1559

Infrared and complex dielectric function studies of $LiNbO_3$ in niobate glass-ceramics

E. F. DE ALMEIDA, J. A. C. DE PAIVA, A. S. B. SOMBRA
Laboratório de Óptica Não-Linear e Ciência dos Materiais (LONLCM), Departamento de Física, Universidade Federal do Ceará, Caixa Postal 6030, 60451-970 -Fortaleza-Ceará-Brazil
E-mail: sombra@ufc.br

Niobate glasses and ceramics [(x Nb_2O_5 $(0.5 - x)$ P_2O_5) 0.5 Li_2O] were prepared by the melt-quenching method and analysed by means of infrared spectroscopy, X-ray powder diffraction and complex impedance methods. $LiNbO_3$ crystals were detected for high niobium content samples. The study of the complex dielectric function of the $LiNbO_3$ ceramics revealed a very broad acoustic resonance mode around 3 MHz. This resonance was associated to the thickness mode of the $LiNbO_3$ plate ceramic resonator. Electrical poling was performed at 300°C for 6 hours under an applied dc potential of 1 kV. Strong changes were observed on the complex dielectric function of the niobate ceramic after the poling. The study of the properties of these ferroelectric ceramics is important in view of possible applications in ultrasonic devices such as delay lines and transducers.

1. Introduction

Recently Komatsu [1] proposed the use of glasses containing ferroelectric crystals such as $LiNbO_3$ as a new type of non-linear optical glass. Lithium niobate, $LiNbO_3$ (LNB), is a ferroelectric material (Curie temperature of 1210°C) with high efficiency for second harmonic generation and is widely used as an optoelectronic device such as in planar waveguides [2]. $LiNbO_3$ crystals also present unusual combinations of ferroelectric, elastic and piezoelectric properties. Successful application of this material in ultrasonic devices, whether as resonators for electromechanical filter applications or as transducers in devices such as ultrasonic delay lines is also reported [3]. Glass *et al.* [4] reported that vitreous $LiNbO_3$ and $LiTaO_3$ were prepared by roller quenching of their liquids and the transparent glasses exhibited dielectric anomalies. The preparation procedure and the study of dielectric, piezoelectric and elastic properties of niobate glasses and ceramics containing $LiNbO_3$ are therefore of interest. In this work a series of lithium niobophosphate glasses [(x $Nb_2O_5{\cdot}(0.5 - x)P_2O_5){\cdot}0.5$ Li_2O], were prepared by the melt quenching technique and studied using infrared spectroscopy (IR), X-ray powder diffraction (XRD) and complex impedance methods. We found that a $LiNbO_3$ ceramic is formed for high niobium concentration ($x = 0.4$ and $x = 0.5$), presenting a resonator mode around 3 MHz for our plate resonator.

2. Experimental procedure

Samples of 15 g each were prepared by mixing appropriate proportion of reagent grade, ammonium phosphate ($NH_4H_2PO_4$), lithium carbonate (Li_2CO_3) and niobium oxide (Nb_2O_5). To prevent excessive boiling and consequent loss of material during melting, water and ammonia in $NH_4H_2PO_4$ were removed by heating the mixture at 200°C for several hours. The mixture was subsequently melted at 1150°C for 1 h in platinum crucibles in an electric furnace. The melt was then poured into a stainless steel mould and pressed between two stainless steel plates. The mould and plates were pre-heated at 300°C. The samples are [(x $Nb_2O_5{\cdot}$ $(0.5 - x)P_2O_5){\cdot}0.5Li_2O$] with x ranging from 0 to 0.5, with increments of 0.1, and are designated by S1 to S6 respectively.

2.1. XRD

The X ray powder diffraction (XRD) patterns were obtained at room temperature (300 K) at a scanning rate of 1 degree minute^{-1} with a Cu-K_α tube at 40 KV and 25 mA using the geometry of Bragg-Brentano.

2.2. IR

The infrared spectra (I.R.) were measured using KBr pellets made from a mixture of powder for each glass composition. The pellet thickness varied from 0.5 to 0.6 mm. The IR spectra were measured from 400 to 1400 cm^{-1} with a NICOLET 5ZPX FT-IR spectrometer.

2.3. Complex dielectric function

The complex dielectric function measurements were done in a HP 4291A Impedance Material Analyzer in conjunction with a HP 4194 A Impedance Analyzer, which jointly cover the region of 100 Hz to 1.8 GHz. The LNB crystals were grown by the Czochralski method in air in platinum crucibles [5]. We used $LiNbO_3$ crystals in Z-cut (LNB Z) and Y-cut geometries (LNBY) (with dimensions $10 \times 10 \times 1$ and

$10 \times 10 \times 1.4$ mm^3 respectively). Samples S1 to S6 have dimensions of $10 \times 10 \times 1.4$ mm^3. All the electrical measurements (including poling) were done with the electrode (silver paste electrode) placed over the highest area of the plate (for the Z-cut LNB crystal the electrode surface is perpendicular to the *z* axis, and for the Y cut, it is perpendicular to the *y* axis).

Electrical poling was performed in the ceramic sample (S6). The sample was heated at 300°C for 2 hours in an electric furnace under applied dc potential of 1 kV in a high vacuum environment (10^{-6} mbar of pressure). Then the temperature was decreased to room temperature while the voltage was held constant. The applied dc field was removed after the sample was cooled to room temperature. The same sample was submitted for a second poling at 300°C for 4 hours (see Fig. 4).

For the LNB (LNBZ, LNBY), glass (S2), ceramic (S6) (see Fig. 3) and the poled ceramic (see Fig. 4) we are exciting acoustic thickness modes of the resonator plates (see reference 6). A thickness mode of vibration in a plate can be interpreted as a standing wave formed by waves propagating in a direction normal to the major surfaces. The use of thickness modes has the advantage that small samples can be used and that the production requirements are reduced to flatness, parallelism, and orientation of the major faces of the sample.

3. Results and discussion

3.1. XRD

According to the XRD (see Fig. 1), samples with *x* ranging between zero to 0.2 show only an amorphous phase, whereas samples with $x > 0.2$ are ceramics. If one increases the niobium concentration, the LNB crystalline phase increases. For sample S6 the lithium niobate is easily identified [7].

3.2. IR spectra

In this work we will use the results of the literature [8, 9] to interpret the IR spectra of the phosphate glasses (see Fig. 2). According to Muller [9], the absorption of the P=O group is around 1282–1205 cm^{-1} in polymeric phosphate chains. The stretching bands of P-O$^-$ (NBO—non-bridging oxygen) are around 1150–1050 and 950–925 cm^{-1}. Absorptions at 800–720 cm^{-1} are due to P-O-P vibrations (BO-bridging oxygen). The bands below 600 cm^{-1} are due to the bending mode of the PO_4 units in phosphate glasses. The spectrum S1 in Fig. 2 shows the IR spectra of the basic lithium niobophosphate glasses. The bands at 1279 cm^{-1} (P=O), 1101 cm^{-1} and 892 cm^{-1} (P-O$^-$), 798 cm^{-1} and 742 cm^{-1} (P-O-P) are present, the bending mode of PO_4 is around 482 cm^{-1}. However with the substitution of P_2O_5 by Nb_2O_5 (Fig. 2), strong changes can be found. The band associated to the bridging oxygen (P-O-P) disappears and a new band around 600 cm^{-1} appears (Fig. 2-S4). The abscence of an infrared absorption band near 1279 cm^{-1} in the glsses S2 and S3 indicates the absence of the the P=O double bond. The band associated to the non bridging oxygen (P-O$^-$) also decreases with the presence of the Nb_2O_5. For samples S4 and S5 where we have the presence of P_2O_5 and Nb_2O_5,

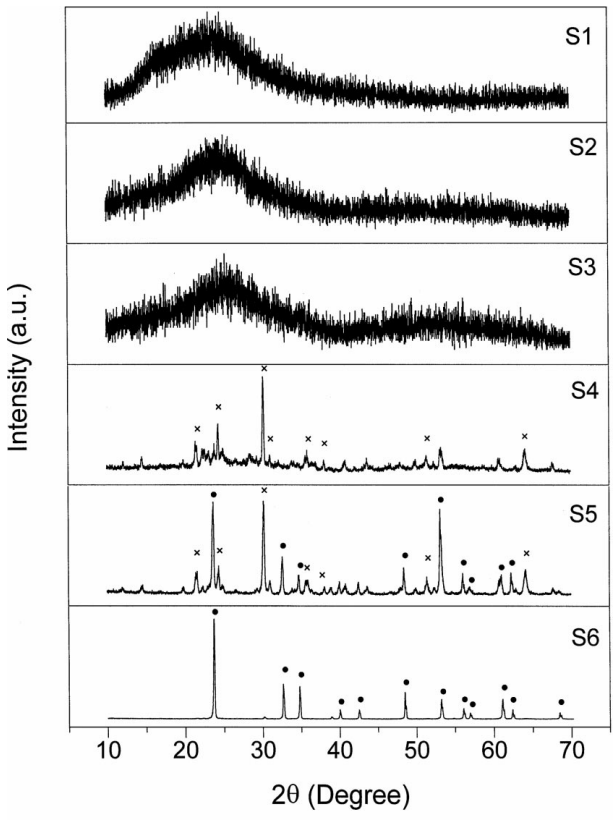

Figure 1 X-ray powder diffraction patterns at room temperature for the samples S1, S2, S3, S4, S5, S6 $\langle (x Nb_2O_5 \cdot (0.5-x) P_2O_5) \cdot 0.5 Li_2O \rangle$ (x = 0, 0.1, 0.2, 0.3, 0.4, 0.5 respectively) ●-$LiNbO_3$, ×-Phosphate phases ($Li_3PO_4 + Li_4P_2O_7 + LiPO_3$).

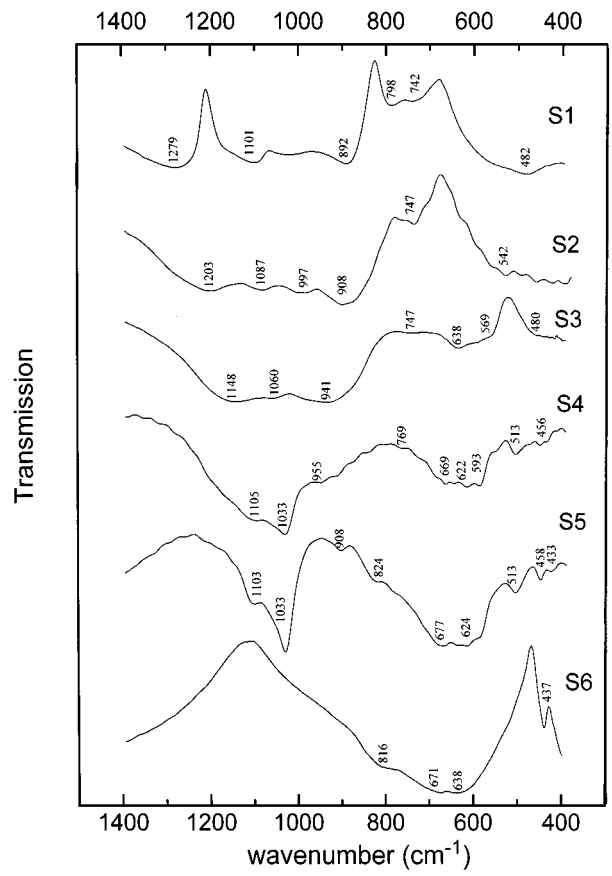

Figure 2 Infrared spectra of the samples S1, S2, S3, S4, S5, S6. The transmission scales have been displaced vertically for clarity.

there are three major absorptions around 1103 cm^{-1}, 1033 cm^{-1} and 620–677 cm^{-1}. The last is probably associated to the formation NbO_6 octahedra. According to the IR data reported in the literature [10], the NbO_6 octahedra present absorption bands around 700 and 610–620 cm^{-1}. In our glass a broad band around 600 cm^{-1} is clear in Fig. 2-S6. The absorptions around 1103 cm^{-1} and 1033 cm^{-1} are associated to the ν_3 antisymmetric stretching vibration of the PO_4 tetrahedra. Results reported in the literature show that the PO_4 tetrahedra, present in crystalline phases like metaphosphatete and orthophosphate, show an absorption mode (ν_3) which is represented by 2 bands of unequal intensity around 1093 cm^{-1} and 1038 cm^{-1} and ν_4 is around 600 cm^{-1} [11]. This doubling of ν_3 may be due to some deformation of the PO_4 tetrahedron, or to vibrational coupling between anions in the same unit cell, or both. The existence of these absorptions in our glass ceramic is an indication of the existence of the crystalline phase containing the PO_4 tetrahedra. In Fig. 2-S6 where we do not have P_2O_5 the absorptions associated to the PO_4 tetrahedra disappear completly. The broad band around 700–600 cm^{-1} in spectra S6 is in entire agreement with the IR spectra of glass-ceramic of $LiNbO_3$ reported in the literature [10]. These reported results show that both glassy and crystalline $LiNbO_3$ exhibit only two absorptions bands at 700 and 610–620 cm^{-1} [10]. These bands have been assigned to the ν_3 mode in the corner-shared NbO_6 octahedron. Fig. 1 shows the XRD of samples S1–S6. In samples S4 and S5 crystalline phases with PO_4 groupings of different degrees of complexity like Li_3PO_4, $Li_4P_2O_7$ and $LiPO_3$ were observed. For the orthophosphate, Li_3PO_4, we have an isolated PO_4^{-3}, two tetrahedra joined for the pyrophosphate, $Li_4P_2O_7$, and long chains and rings of PO_4^{-3} complexes for the methaphosphate, $LiPO_3$. This is in agreement with the IR modes of 1033 and 1103 cm^{-1} for samples S4 and S5 in Fig. 2. If the niobium concentration is increased to $x = 0.4$ the LNB crystalline phase increases. In Fig. 1-S6 the lithium niobate is easily identified [7].

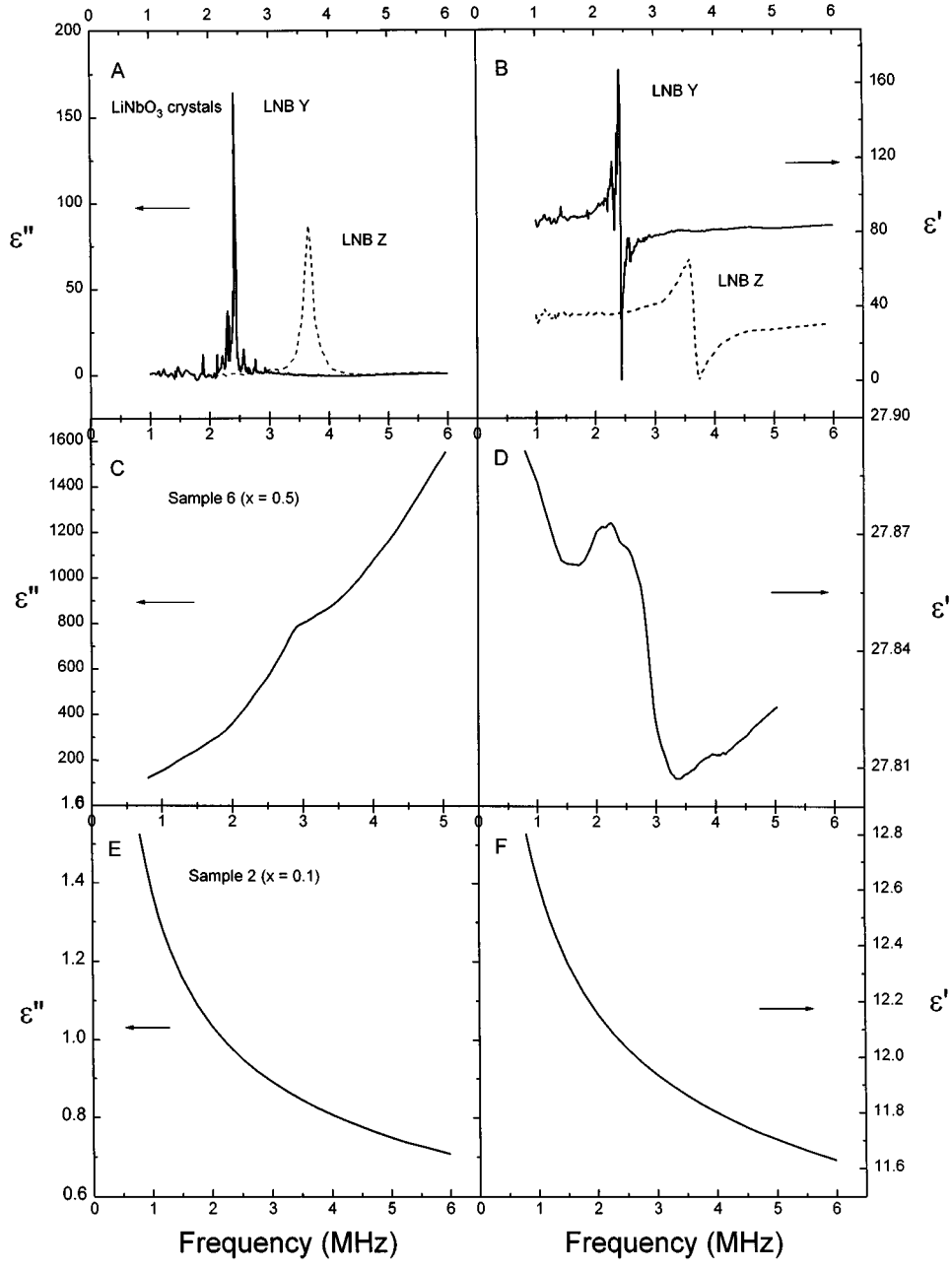

Figure 3 Real (ε') and imaginary (ε'') dielectric functions of the fundamental thickness mode of the samples LNBY, LNBZ, S6 and S2 (See text).

3.3. Complex dielectric function

In Fig. 3A and B one has the imaginary (ε'') and real (ε') dielectric functions of LNBZ and LNBY. One can see the fundamental resonance of thickness mode plate for two LNB orientations. For these resonator geometries one has fundamental frequencies around 2.4 MHz and 3.6 MHz which are in good agreement with the the literature for the parameters of our resonator [5, 6]. For a LNB resonator with 1 mm thickness with different crystal orientations one can find frequency resonances between 1.0 MHz to 4 MHz according to the literature [6]. In the glass resonator (sample S2) one has a very clean behaviour (see Fig. 3E and F). However for the ceramic resonator (see Fig. 3C and D) one can observe a very broad resonance with maximum around 3 MHz for the LNB ceramic resonator. Electrical poling was performed at 300°C for several hours under an applied dc potential of 1 kV, to study the dynamic of this ceramic acoustic resonator. In Fig. 4 one can see that after the second poling procedure, the resonances become more sharp with a short line-width. In Fig. 5 one has the resonances around 3 MHz (sample S62) in an expanded scale. We believe that these resonances are associated with the orientation of electric dipole moments with the poling field. In a recent paper [12], the authors discussed the atomistic origin of the electric dipole moments in a poled lithium based glass. It was proposed that the orientation of electric dipole moments is ascribed to a

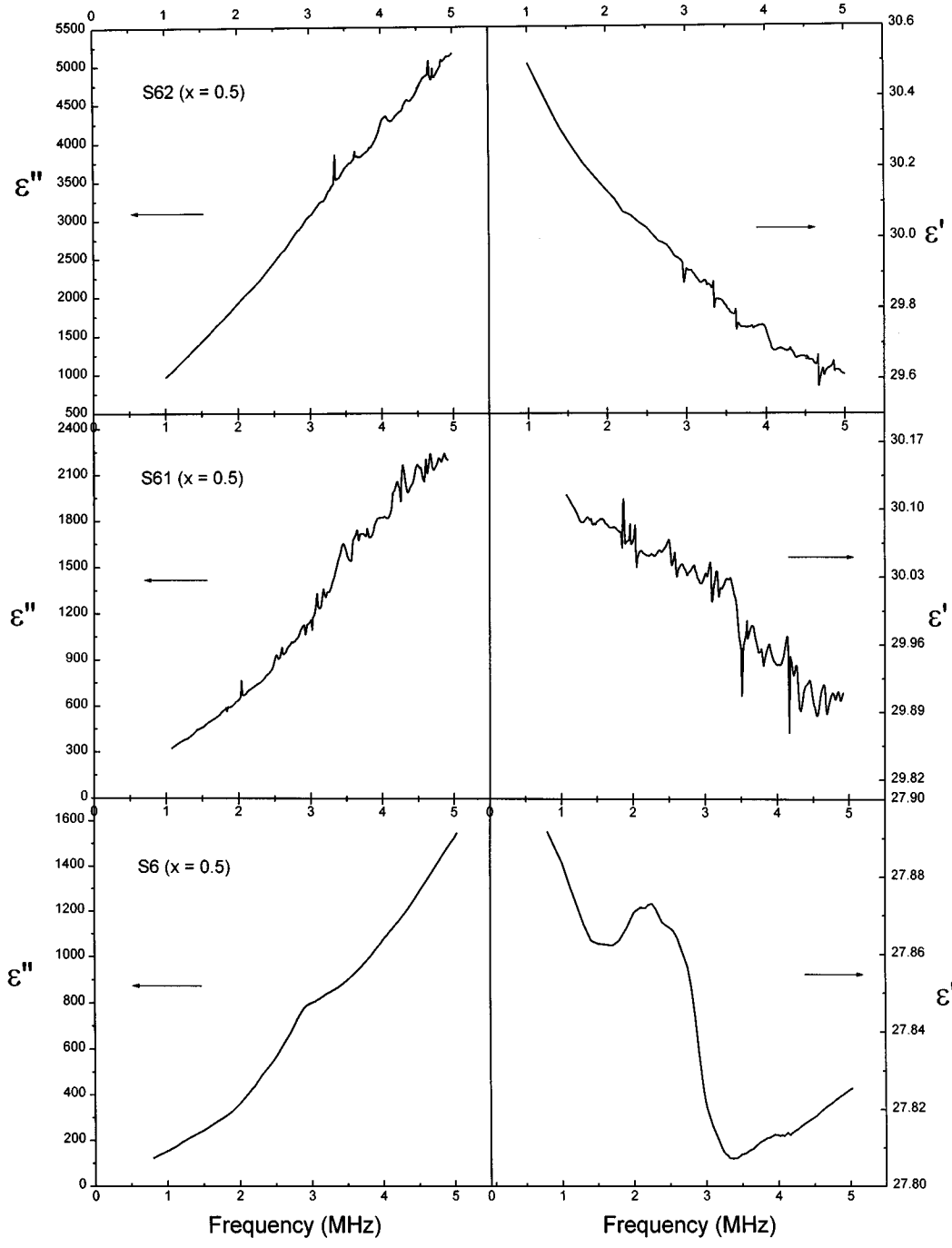

Figure 4 Real (ε') and imaginary (ε'') dielectric functions of the fundamental thickness mode of the samples S6, S61 (S6 with electrical poling performed at 300°C for 2 hours under an applied potential of 1 kV) and S62 (S61 with electrical poling performed at 300°C for 4 hours under applied potential of 1 kV).

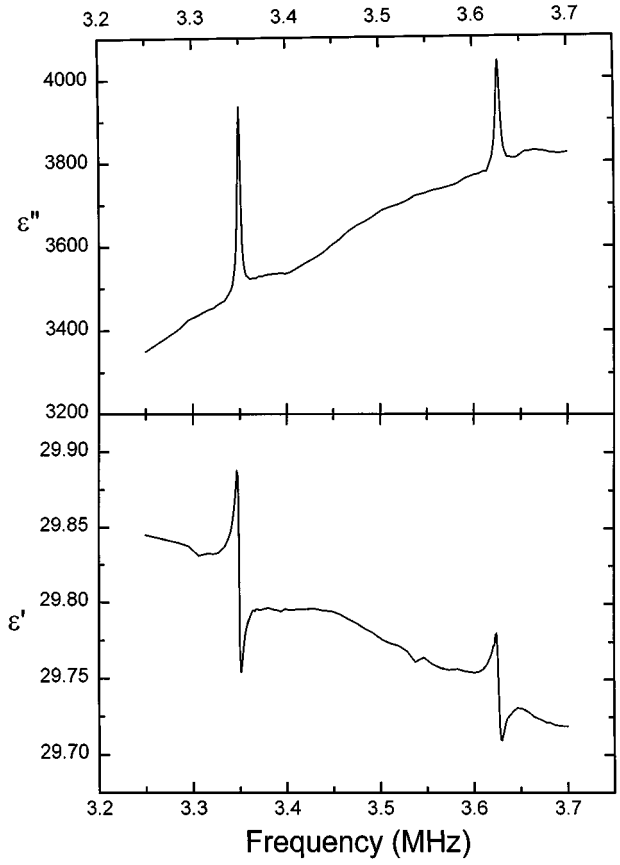

Figure 5 Close-up of the resonances of Fig. 4 (sample S62, $x = 0.5$) around 3 MHz.

migration of Li^+ ions and/or an orientation of structural units of the glass. In our system, the poling process, is increasing the definition of the resonances. The experimental results indicate that the LNB microcrystals is directly associated to the characteristics of the ceramic plate resonator. The possible applications of these materials in ultrasonic devices, whether as resonators for electromecanical filter applications or as transducers in devices such as ultrasonic delay lines, depend upon a knowledge of the complete set of elastic, piezoelectric and dielectric constants as a function of microcrystallite size and distribution over the matrix. The measurement of the elastic and piezoelectric constants of this LNB ceramic, and the control of the size of the microcrystals, will be a necessary step, for a complete understanding of the problem.

4. Conclusion

In conclusion, niobate glasses and ceramics $[(x Nb_2O_5 \cdot (0.5 - x)P_2O_5) \cdot 0.5Li_2O]$ were prepared and the behaviour of $LiNbO_3$ crystals formed in the glass was studied using infrared spectroscopy, X-ray powder diffraction and complex dielectric measurements. The results suggest that crystalline ferroelectric $LiNbO_3$ is formed in samples with high niobium concentration. The study of the complex dielectric function of the LNB ceramics revealed a very broad acoustic resonance mode around 3 MHz for our plate resonator. Strong changes were observed on the complex dielectric function after the electrical poling. The use of these techniques gives new informations about these ferroelectric ceramics in view of possible applications in ultrasonic devices such as delay lines and transducers.

Acknowledgements

This work was partly sponsored by FINEP, FUNCAP, CNPq (Brazilian agencies).

References

1. T. KOMATSU, H. TAWARAYAMA, H. MOHRI and K. MATUSITA, *J. Non-Cryst. Sol.* **135** (1991) 105.
2. M. M. ABOUELLEIL and F. J. LEONBERGER, *J. Am. Ceram. Soc.* **72** (1989) 1311; A. S. B. SOMBRA, *Solid State Comm.* **88** (1993) 305; *Idem., Opt. and Quantum Elect.* **22** (1990) 335.
3. G. S. KINO, "Acoustic Waves, Devices, Imaging and Analog Signal Processing" (Prentice Hall, New Jersey, 1987).
4. A. M. GLASS, M. ELINES, K. NASSAU and J. W. SHIVER, *Appl. Phys. Letters* **31** (1977) 249.
5. J. A. C. DE PAIVA, E. B. DE ARAUJO, A. C. HERNANDES and A. S. B. SOMBRA, *Phys. Stat. Sol.(A)* **147** (1995) 585.
6. A. W. WARNER, M. ONOE and G. A. COQUIN, *J. Acoust. Soc. Am.* **42** (1967) 1223.
7. Joint Commitee on Powder Diffraction Standards (JCPDS), International Center for Diffraction Data, 12 Campus Blvd.; Newton Square, Pensylvania 19073-3723, USA, 1995.
8. A. MOGUS-MILANKOVIC and D. E. DAY, *J. Non-Cryst. Solids* **162** (1993) 275; D. E. C. CORBRIDGE and E. J. LOWE, *J. Chem. Soc. Part I* (1954) 493.
9. K. P. MULLER, *Glastechn. Ber.* **42**(3) (1969) 83.
10. M. TATSUMISAGO, A. HAMADA, T. MINAMI and M. TANAKA, *J. Non-Cryst. Solids* **56** (1983) 423.
11. P. TARTE, *J. Inorg. Nucl. Chem.* **29** (1967) 915.
12. K. TANAKA, K. KASHIMA, K. HIRAO, N. SOGA, A. MITO and H. NASU, *J. Non-Cryst. Sol.* **185** (1995) 123.

Received 19 May 1997
and accepted 30 September 1999